Research Square

Preprints are preliminary reports that have not undergone peer review.
They should not be considered conclusive, used to inform clinical practice,
or referenced by the media as validated information.

In-Vitro Assessment of Multifunctional PGPR Isolated from Pea Plants for Heavy Metal Remediation and Pyrene Biodegradation

Meenakshi Shrivastav
Jiwaji University
Mir Sajad Rabani
Govt. Degree College Doda
Mahendra K. Gupta
mkgsac@yahoo.com

Jiwaji University

Research Article

Keywords: Plant growth promotion, Bioinoculant, Sustainable agriculture, Heavy-metal tolerance, Bioremediation

Posted Date: April 20th, 2026

DOI: https://doi.org/10.21203/rs.3.rs-9271143/v1

License: This work is licensed under a Creative Commons Attribution 4.0 International License.
Read Full License

Additional Declarations: No competing interests reported.

Abstract

Soil contamination by heavy metals and polycyclic aromatic hydrocarbons (PAHs) poses a significant threat to food safety, soil fertility and sustainable agricultural productivity. Plant growth-promoting rhizobacteria (PGPR) provide eco-friendly strategies for enhancing crop growth while mitigating environmental pollutants. Legume associated rhizobacteria are particularly valued for their adaptive resilience under stress conditions. This study evaluated PGPR isolated from the rhizosphere of pea (*Pisum sativum* L.) for heavy metal tolerance and pyrene biodegradation under in-vitro conditions. A total of twenty bacterial isolates were obtained and screened for plant growth promoting traits including indole-3-acetic acid (IAA) production, phosphate solubilization, ammonia production, siderophore production, hydrogen cyanide production and nitrogen fixation potential. Among them, isolates P2B and P3A demonstrated superior multifunctional performance. Isolate P2B exhibited higher IAA production (59.25 µg mL^{-1} at 144 h) and strong siderophore production (88.26% SU), whereas P3A showed enhanced ammonia production and broader metabolic versatility. Both isolates displayed substantial tolerance to Ni, Co, Cr and Cd, with P3A showing greater resistance to cobalt and cadmium. Growth in pyrene amended media revealed concentration dependent adaptation and efficient biodegradation, achieving 99% and 98% pyrene degradation after 21 days by P2B and P3A, respectively. Biochemical characterization and 16S rRNA gene sequencing identified the isolates as *Pseudomonas glycinae* (P2B) and *Priestia aryabhattai* (P3A). The combined expression of plant growth promoting traits, multi-metal tolerance and pyrene degradation capacity highlights these strains as promising multifunctional bioinoculants for sustainable bioremediation of contaminated agricultural soils.

1. Introduction

Soil root interfaces host diverse microbial communities that strongly influence plant health, nutrition, and stress resilience. Plant growth promoting rhizobacteria enhance plant performance through multiple mechanisms like phytohormone (e.g., IAA) production, nutrient solubilization (phosphate, zinc), siderophores mediated iron acquisition and metabolites such as hydrogen cyanide (HCN) and ammonia that can suppress phytopathogens making them attractive as eco-friendly bioinoculants for sustainable agriculture [1, 2]. Legumes such as pea actively shape their rhizosphere microbiome via root exudates, recruiting bacteria that assist nutrient uptake and stress mitigation. Rhizosphere communities frequently show enrichment of genes related to metal resistance and plant beneficial functions, indicating that legume-associated bacteria are promising sources of multifunctional PGPR [3]. Concurrently, agricultural soils are increasingly affected by co-contamination from heavy metals (e.g., Cr, Cd, Ni and Co) and persistent organic pollutants such as polycyclic aromatic hydrocarbons (PAHs). Heavy metals impair plant physiology and microbial activity, while PAHs like pyrene are recalcitrant, toxic and pose food-safety risks [4, 5]. Microbial strains that combine plant growth promotion with tolerance to or transformation of such contaminants provide a dual benefit solution. They can support crop productivity while contributing to in-situ bioremediation [6, 7]. Mechanistically, PGPR can alleviate metal stress via biosorption, efflux, sequestration and by stimulating plant antioxidant systems; likewise many soil bacteria metabolize PAHs through oxygenase-mediated pathways, often achieving substantial PAHs

removal under aerobic conditions or when aided by consortia and bio-augmentation strategies [8–10]. These trait combinations such as PGP activities, multi-metal tolerance (measured as MICs) and PAH-degrading capacity are therefore valuable selection criteria when prospecting rhizosphere isolates for field applications. This study evaluates the potential of twenty bacterial strains isolated from pea rhizosphere and evaluates classical PGP traits (IAA, phosphate and zinc solubilization, siderophore, HCN, ammonia), heavy-metal tolerance (Ni, Co, Cr, Cd) and biodegradation of pyrene. Two high-performing isolates were further identified by 16S rRNA sequencing. By documenting multifunctional isolates from pea rhizosphere, we aim to expand the pool of candidate bioinoculants able to support plant growth and remediate metal and PAHs contaminated soils.

2. Materials and methods

2.1 Study area and site description

Rhizospheric soil samples were collected from cultivated pea (*Pisum sativum* L.) fields located in five different sites in Gwalior-Bhind region, Madhya Pradesh, India. The study area lies between geographical coordinates of 26.21°-26.34° N latitude and 78.12°-78.48° E longitude, at an average elevation of approximately 196 m (Gwalior) and 164 m (Bhind) above mean sea level. This area falls under the semi-arid agro-climatic zone of central India and experiences a subtropical climate with hot summers, moderate monsoon rainfall and mild winters.

2.2 Sample collection and isolation of rhizobacteria

Rhizospheric soil samples were collected from healthy *Pisum sativum* plants at the flowering stage from various field locations of the study area by following the method put forward by [11]. Healthy pea plants at the flowering stage were randomly selected from cultivated fields to ensure active rhizosphere microbial activity. Plants showing no visible symptoms of disease or stress were carefully uprooted and loosely adhering soil was removed. Soil tightly attached to the roots (approx. 5–15 cm depth) was collected in sterile polythene bags, stored at 4°C and transferred to Microbiology Research Laboratory at School of studies in Botany, Jiwaji University Gwalior and processed for microbial analysis within 24 h. One gram of soil was suspended in 9 mL of sterile 0.85% saline and serially diluted (10^{-1} to 10^{-10}). Aliquots (100 µL) of dilutions were spread on Nutrient Agar (NA) plates and incubated at 30 ± 2°C for 24–48 h. Morphologically distinct colonies were picked, purified by repeated streaking and stored as glycerol stocks (20%) at -30°C.

2.3 Screening of plant growth promoting traits

All twenty bacterial isolates were evaluated for their plant growth promoting attributes, which include the production of indole-3-acetic acid, phosphate solubilization, siderophore production, hydrogen cyanide formation, ammonia production and zinc solubilization. Each assay was performed in triplicate under sterile laboratory conditions.

2.3.1 Indole-3-acetic acid production

IAA production was quantified following the method of [12], with minor modifications. Bacterial isolates were grown in Luria-Bertani (LB) broth supplemented with 0.05 g L^{-1} L-tryptophan and incubated at 28 ± 2°C for 144 h under shaking conditions (120 rpm). After incubation, the culture was centrifuged at 10,000 rpm for 10 min and 2 mL of supernatant was mixed with 4 mL of Salkowski reagent (1 mL 0.5 M $FeCl_3$ in 50 mL 35% perchloric acid). The development of a pink coloration after 30 min of incubation at room temperature indicated IAA production and the absorbance of the solution was measured at 530 nm using a UV-Vis spectrophotometer. IAA concentration was determined using a standard curve of pure IAA [12, 13].

2.3.2 Phosphate solubilization

Phosphate solubilization ability was determined using Pikovskaya's agar medium containing insoluble tricalcium phosphate as described by [14]. Each isolate was spot-inoculated on the agar plates and incubated at 28°C for 5–7 days. The appearance of a clear halo zone surrounding the colonies indicated phosphate solubilization. The solubilization index (SI) was calculated as the ratio of total diameter (colony+halo) to colony diameter [15]. Quantitative estimation of phosphate solubilization was carried out at different time intervals following the method described by [16] with modifications. The quantity of solubilized phosphorus was determined by using a calibration curve of potassium dihydrogen phosphate (KH_2PO_4).

2.3.3 Siderophore production

Siderophore production was assayed qualitatively using the Chrome Azurol S (CAS) agar diffusion method [17]. Bacterial isolates were spot inoculated onto CAS agar plates and incubated at 28 ± 2°C for 5 days. Development of an orange, orange yellow or a clear halo around the colony against the blue background indicated siderophore production. The quantitative estimation was done by CAS-liquid assay. Briefly, 1 mL of cell free supernatant was mixed with 1 mL CAS solution. The absorbance of the color obtained was measured using the spectrophotometer at 630 nm. The percentage of siderophore units was estimated using the formula (% Siderophore units= [(Ar - As)/Ar] x 100), where Ar is the absorbance at 630 nm of reference (CAS assay solution+uninoculated media) and As is the absorbance at 630 nm of the sample (CAS assay solution+supernatant) [18].

2.3.4 Hydrogen cyanide production

HCN production was tested using the method of [19]. Nutrient agar plates were supplemented with 4.4 g L^{-1} glycine for detection of HCN. A Whatman No. 1 filter paper soaked in 0.5% picric acid solution (in 2% sodium carbonate) was placed in the upper lid of the Petri dish, and the plates were sealed with parafilm to prevent gas leakage. After 4 days of incubation at 28°C, a colour change of the filter paper from yellow to reddish-brown indicated positive HCN production.

2.3.5 Ammonia production

Ammonia production was tested according to [20]. Each isolate was inoculated into 10 mL of peptone water and incubated at 28°C for 48 h. After incubation the medium was centrifuged for 5 min, then 1 mL of supernatant was collected in a fresh test tube and 2 mL of Nessler's reagent was added to each tube, then the final volume was adjusted to 10 mL by adding distilled water. The development of a yellow to brown colour indicated ammonia production and intensity of the color was measured using spectrophotometer at 450 nm.

2.3.6 Zinc solubilization

Zinc solubilization was assessed following the modified method of [21]. The isolates were spot-inoculated onto Zinc solubilizing agar medium containing 0.1% zinc oxide (ZnO) or zinc carbonate ($ZnCO_3$) as an insoluble zinc source. Plates were incubated at 28°C for 7 days and clear halos around the colonies indicated zinc solubilization. Zinc solubilization index (ZSI) was calculated similarly to that of phosphate soubilization index (PSI).

2.3.7 Nitrogen (N_2) fixation

Nitrogen fixation ability of the selected bacterial isolates was qualitatively assessed using Burk's nitrogen-free agar medium, which supports the growth of only those microorganisms capable of fixing atmospheric nitrogen [22].

2.3.8 Pectinase, lipase and cellulase production

The in-vitro production of pectinase, lipase and cellulase by bacterial isolates was screened using substrate specific plate assays. Pectinase activity was assessed on pectin agar plates, where clear zones after CTAB flooding indicated enzyme production. Lipase activity was determined on tributyrin agar by the formation of halo zones around colonies. Cellulase production was evaluated on CMC agar plates, where clear zones after flooding with iodine solution confirmed cellulose degradation. The clear hydrolysis zones around the colony were used as an indicator of enzymatic activity [23–25].

2.4 Heavy metal tolerance and minimum inhibitory concentration (MIC)

The isolates were tested for tolerance to nickel (Ni), cobalt (Co), chromium (Cr) and Cadmium (Cd). Metal salts (e.g., $NiCl_2$, $CoCl_2$, $K_2Cr_2O_7$ and $CdCl_2$) were incorporated into LB agar at increasing concentrations (25, 50 & 100 μg mL^{-1}) by well diffusion method. Plates were surface inoculated (10^6 CFU mL^{-1} suspensions, 50 μL) with the help of sterilized cotton swabs before the addition of metal salts and incubated at 28°C for 72 h. The highest concentration that inhibited the visible growth was recorded as the MIC for that metal for each isolate [26].

2.5 Growth analysis of rhizobacterial isolates in pyrene amended medium

The growth response of selected rhizobacterial isolates was evaluated in mineral salt medium (MSM) supplemented with pyrene as the sole carbon and energy source. Pyrene stock solution was prepared in analytical-grade acetone and added aseptically to sterile MSM to obtain final concentrations of 50, 100 and 150 mg L^{-1}. The solvent was allowed to evaporate under sterile conditions prior to inoculation to avoid solvent toxicity. Each flask containing 100 mL MSM was inoculated with 1% (v/v) bacterial culture adjusted to an optical density (OD 600) of approximately 0.1. Uninoculated controls were maintained under identical conditions. Cultures were incubated at 30 ± 2°C under shaking conditions (120 rpm) to ensure adequate aeration and hydrocarbon availability. Bacterial growth was monitored at 7, 14 and 21 days by measuring optical density at 600 nm using a UV-Vis spectrophotometer (Schimadzu, UV-1800). All experiments were conducted in triplicate and results were expressed as mean ± standard deviation [27].

2.6 Pyrene biodegradation assay

The selected isolates were assessed for degradation of pyrene. The assay was carried out in Minimal Salt Medium (MSM) containing 100 mg L^{-1} of the PAH (dissolved in acetone, allowed to evaporate). Bacterial cells (1×10^7 CFU mL^{-1}) were inoculated, incubated at 30°C, 120 rpm for 21 days. Controls without inoculum were included. The residual pyrene was extracted with hexane and concentration was measured via UV-Vis Spectrophotometer at 335 nm. The percentage degradation was calculated using a standard curve (10–100 mg L^{-1}) [28, 29].

2.7 Biochemical characterization and sugar fermentation assays

Biochemical characterization of the bacterial isolates (P2B and P3A) was performed using standard microbiological procedures to determine their metabolic and enzymatic properties. The biochemical tests were conducted according to standard protocols described in Bergey's Manual of Determinative Bacteriology and Cappuccino and Sherman [30, 20]. Carbohydrate fermentation patterns were determined using phenol red carbohydrate fermentation broth containing individual sugars (glucose, fructose, maltose, mannitol, mannose, inositol, rhamnose, raffinose, xylose, and inulin) supplemented with Durham tubes for gas detection. Each isolate was inoculated aseptically into sterilized fermentation media and incubated at 37 ± 2°C for 24–48 h. A colour change from red to yellow indicated acid production due to sugar fermentation. Gas production, when present was recorded by bubble formation in Durham tubes. Absence of colour change indicated negative fermentation. All biochemical and fermentation tests were performed in triplicate to ensure reproducibility and accuracy of results [20].

2.8 Molecular identification via 16S rRNA sequencing

The two best performing isolates based on PGP, heavy metal tolerance and pyrene degradation were selected for molecular identification by 16S rRNA gene Sanger sequencing. Genomic DNA was extracted using a standard CTAB method. The 16S rRNA gene was amplified using universal primers (707 R and 704 F). PCR conditions included initial denaturation at 95°C for 5 min; 35 cycles of 95°C for 30 s, 55°C

for 30 s, 72°C for 90 s; final extension at 72°C for 10 min. PCR products were purified, sequenced bidirectionally, trimmed and compared to the NCBI GenBank database via nucleotide BLAST. Phylogenetic tree was constructed using MEGA 11 by neighbor joining method with 1000 bootstrap replications [31].

2.9 Data analysis

All experiments were conducted in triplicate. Quantitative data (e.g., IAA production, halo diameters, MIC values, % PAH degradation) were expressed as mean ± standard deviation. Origin, 2018 and Microsoft excel, 2013 were used for analysis.

3. Results and discussion

3.1 Isolation and morphological characterization of rhizobacterial isolates

Rhizobacterial isolates were successfully isolated from the rhizosphere soil of pea plants using serial dilution and spread plate techniques. The results obtained for physicochemical analysis are presented in Table 1. A total of twenty morphologically distinct bacterial isolates were obtained from five different sites of Gwalior and Bhind region (Table 1), based on differences in colony appearance on nutrient agar media. These isolates were further purified by repeated streaking to obtain single, uniform colonies. Preliminary morphological characterization revealed considerable diversity among the isolates in terms of colony size, shape, margin, elevation, color, and surface texture. Among the twenty isolates, two promising strains designated P2B and P3A were selected for detailed characterization based on their superior performance in preliminary plant growth promoting and stress tolerance assays. Isolate P2B formed small-medium, circular colonies with smooth surfaces, entire margins and creamy-white pigmentation. Microscopic examination revealed Gram-negative, rod-shaped cells, typical of *Pseudomonas* species. In contrast, isolate P3A produced large, circular, yellowish colonies with smooth surfaces and entire margins (Table 2). The cells were Gram-positive, rod-shaped and consistent with characteristics of the genus *Priestia*. These morphological features corroborated the molecular identification of both isolates and supported their selection for further functional studies.

Table 1
Sample sites and physicochemical parameters of soil samples

Sample Sites	pH (Units)	Temp. (\varvec C)	EC (μs cm^{-1})	N	P	K	Isolate codes
				($mg\ Kg^{-1}$)			
Barthara Village, Gohad, Bhind, 477116	7.72 ± 0.07	21	241	88.33	44.60	1804	P1a, P1b, P1c, P1d
Near Vaisali Dam, Gwalior Road, Bhind, 477116	7.67 ± 0.05	21	242	60.30	40.40	2208	P2a, P2b, P2c, P2d
Botanical Garden, Jiwaji University, Gwalior, 474011	7.37 ± 0.07	22	215	67.60	49.20	2356	P3a, P3b, P3c, P3d
Sirol Village, Gwalior, 474006	7.42 ± 0.04	20	208	94.6	46.80	2485	P4a, P4b, P4c
Khureri Village, Badagaon, Gwalior, 474006	7.59 ± 0.06	36	288	78.3	41.60	2734	P5a, P5b, P5d, P5e, P5f

Table 2
Morphological characteristics of selected rhizobacterial isolates

Morphological Characteristic	P2B (*Pseudomonas glycinae*)	P3A (*Priestia aryabhattai*)
Colony morphology	Circular, smooth, flat	Circular, large, opaque
Colony color	Cream to pale white	White to off-white
Margin	Entire	Entire
Elevation	Flat	Slightly raised
Cell shape	Rod-shaped	Rod-shaped
Gram reaction	Gram-negative	Gram-positive
Motility	Motile	Motile
Spore formation	Non-spore forming	Endospore forming

3.2 Screening and estimation of PGP traits

Both isolates tested positive for several key PGP traits, including indole-3-acetic acid production, phosphate solubilization, ammonia production, zinc solubilization, siderophore production, nitrogen fixation, HCN production and extracellular enzyme activities such as pectinase, lipase and cellulase. The

presence of diverse enzymatic activities suggests a strong capacity of the isolates to contribute to nutrient cycling, root colonization and plant microbe interactions.

3.2.1 Indole-3-acetic acid production

Quantitative estimation of IAA production revealed a time dependent increase in both isolates (Table 3). Isolate P2B exhibited significantly higher IAA production compared to P3A at all incubation periods. P2B produced 12.58, 56.63, and 59.25 µg mL^{-1} of IAA after 48, 96 and 144 h, respectively. In contrast, isolate P3A produced comparatively lower amounts of IAA, measuring 4.08, 6.38 and 22.29 µg mL^{-1} at the same respective time intervals. The results indicate superior auxin producing capability of isolate P2B.

3.2.2 Phosphate solubilization

Phosphate solubilization index was found to be 2.86 for P2B and 2.80 for P3A. Phosphate solubilization potential varied between the two isolates and increased with incubation time. Isolate P2B solubilized 48.49, 44.47 and 64.40 µg mL^{-1} of phosphate at 72, 120 and 168 h, respectively. Isolate P3A showed solubilization values of 32.42, 36.78 and 81.04 µg mL^{-1} at the corresponding time intervals. Notably, P3A exhibited the highest phosphate solubilization at 168 h, suggesting delayed but enhanced solubilization efficiency compared to P2B.

3.2.3 Ammonia production

Ammonia production assay showed that both isolates were capable of releasing appreciable amounts of ammonia after 48 h of incubation. Isolate P2B produced 21.62 µg mL^{-1}, whereas isolate P3A produced a significantly higher amount measuring 62.36 µg mL^{-1}, indicating stronger nitrogen metabolism potential in P3A.

3.2.4 Siderophore production

Siderophore production, expressed as siderophore units (% SU), was evaluated for isolate P2B and P3A. The isolate P2B exhibited substantial siderophore production, yielding 67.28% SU, while as isolate P3A exhibited 88.26% SU. The high siderophore production of P3A indicates an enhanced ability of the isolate to chelate iron, which is crucial for plant growth promotion and metal stress alleviation (Table 3).

3.2.5 HCN production

Hydrogen cyanide (HCN) production was detected only in isolate P2B, while isolate P3A was found negative for HCN production (Fig. 1).

3.2.6 Zinc solubilization

Zinc solubilization was detected on the basis of clear zone formation around the bacterial colony. Bacterial isolates were found positive for zinc solubilization with ZSI for P2B as 2.62 and 2.67 P3A (Fig. 1).

3.2.7 N_2 fixation

Both the isolates were found positive for N_2 fixation based on visible growth on Burk's Medium.

3.2.8 Pectinase, lipase and cellulase production

Bacterial isolate P2B and P3A were found positive for in-vitro pectinase, lipase and cellulase production.

Table 3
Qualitative and quantitative PGP traits exhibited by selected rhizobacterial isolates

	PGP Trait	Parameter / Unit	P2B	P3A
Quantitative study	Indole-3-acetic acid (IAA) production	µg mL^{-1} (48 h)	12.58	4.08
		µg mL^{-1} (96 h)	56.63	6.38
		µg mL^{-1} (144 h)	59.25	22.29
	Phosphate solubilization	µg mL^{-1} (72 h)	48.49	32.42
		µg mL^{-1} (120 h)	44.47	36.78
		µg mL^{-1} (168 h)	64.40	81.04
	Ammonia production	µg mL^{-1} (48 h)	21.62	62.36
Qualitative study	Siderophore production	% Siderophore Units (% SU)	67.28	88.26
	Phosphate solubilization (qualitative)	Pikovskaya's agar	+	+
	Phosphate solubilization index (PSI)	-	2.86	2.80
	Zinc solubilization	Agar plate assay	+	+
	Zinc solubilization index (ZSI)	-	2.62	2.67
	Nitrogen fixation	Growth on N_2-free (Burk's) medium	+	+
	HCN production	Picrate assay	+	–
	Pectinase activity	Plate assay	+	+
	Lipase activity	Plate assay	+	+
	Cellulase activity	Plate assay	+	+

Note: "+" indicates positive reaction; "–" indicates negative reaction.

3.3 Heavy metal tolerance of rhizobacterial isolates

The heavy metal tolerance of the selected rhizobacterial isolates was evaluated by determining the minimum inhibitory concentration (MIC) against nickel (Ni), cobalt (Co), chromium (Cr), and cadmium

(Cd). Both isolates exhibited considerable tolerance to all tested metals, although variations in resistance levels were observed. Isolates P2B and P3A showed similar tolerance to nickel and chromium with MIC values of 50 µg mL^{-1} for both metals indicating comparable resistance to these elements. Notably, isolate P3A demonstrated higher tolerance to cobalt, exhibiting growth up to 150 µg mL^{-1} concentration of cobalt, compared to 100 µg mL^{-1} observed for isolate P2B. In contrast, isolate P2B showed lower tolerance to cadmium with an MIC value of 25 µg mL^{-1}, whereas P3A displayed substantially greater resistance, sustaining growth at cadmium concentrations as high as 50 µg mL^{-1} (Table 4). Overall, the results indicate that both isolates possess strong heavy metal tolerance with P3A exhibiting superior resistance to cobalt, suggesting its enhanced suitability for application in metal-contaminated environments.

Table 4
Minimum inhibitory concentration (MIC) of heavy metals for selected rhizobacterial isolates (µg ml^{-1})

Isolate	Nickel	Cobalt	Chromium	Cadmium
P2B	50 µg mL^{-1}	100 µg mL^{-1}	50 µg mL^{-1}	25 µg mL^{-1}
P3A	50 µg mL^{-1}	150 µg mL^{-1}	50 µg mL^{-1}	50 µg mL^{-1}

3.4 Growth assay of isolates in pyrene amended medium

The growth response of P2B and P3A was evaluated in pyrene amended mineral medium at concentrations of 50, 100 and 150 mg L^{-1} over an incubation period of 21 days (Table 5). Bacterial growth showed clear variation depending on both pyrene concentration and incubation time. At 50 mg L^{-1} pyrene, both isolates exhibited the highest growth throughout the experimental period. Growth increased progressively with time indicating effective adaptation and utilization of pyrene. In P2B, growth values increased from 0.47 ± 0.03 at day 7 to 0.79 ± 0.02 at day 14 and reached a maximum of 1.18 ± 0.05 by day 21. Similarly, P3A showed an increase from 0.38 ± 0.02 (day 7) to 0.73 ± 0.03 (day 14) and 1.06 ± 0.04 at day 21. The significant increase across incubation time indicates active metabolism and efficient tolerance to lower pyrene concentration. At 100 mg L^{-1}, bacterial growth was comparatively reduced but still increased steadily over time. P2B showed growth values of 0.32 ± 0.02, 0.61 ± 0.03, and 0.97 ± 0.04 at 7, 14, and 21 days, respectively. P3A followed a similar trend with slightly lower values (0.27 ± 0.02, 0.58 ± 0.02, and 0.88 ± 0.03). This suggests moderate inhibition at higher pyrene concentration while maintaining metabolic activity. At the highest concentration (150 mg L^{-1}), growth of both strains was markedly suppressed. Initial growth at day 7 was minimal (0.14 ± 0.01 for P2B and 0.11 ± 0.01 for P3A). Although growth increased by day 14 (0.43 ± 0.03 and 0.33 ± 0.02, respectively), no further significant increase was observed at day 21, indicating possible toxic effects of elevated pyrene levels that limited further bacterial proliferation. Overall, growth decreased with increasing pyrene concentration but increased with incubation time, demonstrating concentration dependent inhibition and time-dependent adaptation. Between the two isolates, *Pseudomonas glycinae* (P2B) consistently exhibited slightly higher growth than *Priestia aryabhattai* (P3A), suggesting comparatively greater tolerance and potential efficiency in pyrene degradation under stressed conditions. The statistical

grouping indicated by different superscript letters confirms significant differences among treatments at $p \leq 0.05$.

3.5 Pyrene degradation

The results demonstrated a time dependent increase in pyrene degradation by both bacterial isolates, P2B and P3A. At 7 days of incubation, isolate P2B exhibited 58% degradation of pyrene with 42% residual concentration, whereas P3A showed comparatively lower degradation of 50% with 50% residual pyrene. A substantial increase in degradation efficiency was observed at 14 days, where P2B achieved 92% degradation leaving only 8% residual pyrene, while P3A degraded 88% with 12% remaining. By 21 days of incubation, both isolates showed near-complete degradation, with P2B reaching 99% degradation (1% residual) and P3A achieving 98% degradation (2% residual). Overall, isolate P2B consistently demonstrated slightly higher degradation efficiency than P3A at all incubation periods, indicating its superior potential for pyrene bioremediation.

Table 5
Growth response of P2B and P3A in pyrene amended mineral medium at concentrations of 50, 100, and 150 mg L^{-1} over 21 days of incubation

Pyrene (mg L^{-1})	**Time (Days)**	**P2B (*Pseudomonas glycinae*)**	**P3A (*Priestia aryabhattai*)**
50	7	0.47 ± 0.03	0.38 ± 0.02
	14	0.79 ± 0.02	0.73 ± 0.03
	21	1.18 ± 0.05	1.06 ± 0.04
100	7	0.32 ± 0.02	0.27 ± 0.02
	14	0.61 ± 0.03	0.58 ± 0.02
	21	0.97 ± 0.04	0.88 ± 0.03
150	7	0.14 ± 0.01	0.11 ± 0.01
	14	0.43 ± 0.03	0.33 ± 0.02
	21	0.43 ± 0.03	0.33 ± 0.02

Values represent mean ± standard deviation of three independent replicates (n = 3). Different superscript letters within each column indicate statistically significant differences according to one-way ANOVA followed by Tukey's HSD test at $p \leq 0.05$.

Table 6
Pyrene degradation efficiency and residual concentration by selected rhizobacterial isolates

Isolate	Incubation Time (days)	Pyrene Degradation (%)	Residual Pyrene Concentration (%)
P2B	7	58	42
	14	92	8
	21	99	1
P3A	7	50	50
	14	88	12
	21	98	2

3.6 Biochemical characterization

Biochemical profiling revealed distinct metabolic characteristics between the two isolates (Table 2). Both isolates were positive for gelatinase, catalase, urease, citrate, nitrate activity and growth in 6.5% NaCl, indicating enzymatic versatility and tolerance to saline conditions. Isolate P2B was also positive for oxidase and esculin hydrolysis while being negative for indole, methyl red voges-proskauer and starch hydrolysis. In contrast, P3A was positive for voges-proskauer, citrate utilization and starch hydrolysis, while being negative for oxidase, indole, methyl red and esculin hydrolysis. These biochemical differences suggest taxonomic and functional diversity between the isolates.

Sugar fermentation assays further differentiated the isolates. Isolate P2B fermented fructose and mannitol, while remaining negative for all other tested sugars. Conversely, P3A showed a broader carbohydrate utilization pattern, fermenting glucose, inositol, mannitol and mannose, but was negative for maltose, inulin, inositol, rhamnose, raffinose and xylose. The wider substrate utilization by P3A indicates greater metabolic flexibility.

Table 7
Biochemical characteristics of selected rhizobacterial isolates

Biochemical Characteristic	P2B (*Pseudomonas glycinae*)	P3A (*Priestia aryabhattai*)
Catalase test	Positive	Positive
Oxidase test	Positive	Negative
Indole production	Negative	Negative
Methyl Red (MR)	Negative	Negative
Voges–Proskauer (VP)	Negative	Positive
Citrate utilization	Positive	Positive
Starch hydrolysis	Negative	Positive
Gelatin production	Positive	Positive
Nitrate reduction	Positive	Positive
Urease	Positive	Positive
Esculin hydrolysis	Positive	Negative
Growth at 6.5% NaCl	Positive	Positive

3.7 Molecular identification of promising rhizobacterial isolates

The two promising rhizobacterial isolates, P2B and P3A were identified using 16S rRNA gene sequencing. The amplified 16S rRNA gene sequences were analyzed and compared with reference sequences available in the NCBI GenBank database using BLAST. Isolate P2B exhibited a high level of sequence similarity with *Pseudomonas glycinae* strain MS586 (99.73%), while isolate P3A showed close affiliation with *Priestia aryabhattai* B8W22 (99.86%) (Table 8). The phylogenetic tree was constructed for both the strains by neighbour joining method using MEGA11 (Figs. 4 & 5). The molecular identification confirmed the taxonomic identity of both isolates and is consistent with their observed plant growth promoting traits, heavy metal tolerance and pyrene biodegradation potential. These findings further validate the suitability of *P. glycinae* P2B and *P. aryabhattai* P3A for application in sustainable agriculture and bioremediation of contaminated soils.

Table 8
Bacterial strains with accession numbers and type strains showing highest similarity

Isolate	Identified bacterial strain	Accession number	Type strain with highest percentage of similarity
P2B	*Pseudomonas glycinae* strain MSP2B	PZ225431	NR_179889.1:21-1492 *Pseudomonas glycinae* strain MS586 (99.73%)
P3A	*Priestia aryabhattai* strain MSP3A	PZ225442	NR_115953.1:16-1472 *Priestia aryabhattai* B8W22 (99.86%)

4. Discussion

In the present study, among the twenty rhizobacterial isolates, two most potent bacterial isolates designated P2B and P3A demonstrated a combination of plant growth promoting attributes, tolerance to heavy metals and a high capacity for pyrene degradation. Morphological characterization revealed that isolate P2B exhibited traits typical of *Pseudomonas* sp., while P3A showed morphological features consistent with *Priestia* sp., characterized by large, opaque colonies and Gram-positive rods. These phenotypic observations were further confirmed by 16S rRNA gene sequencing, which identified P2B as *Pseudomonas glycinae* strain MSP2B and P3A as *Priestia aryabhattai* strain MSP3A. The congruence between morphological and molecular identification strengthens the taxonomic reliability of the isolates and aligns with earlier reports highlighting *Pseudomonas* and *Priestia* species as effective rhizosphere competent bacteria with diverse PGP functions. Both isolates expressed multiple PGP traits, including IAA production, phosphate and zinc solubilization, ammonia production and siderophore synthesis underscoring their multifunctional nature. Such traits are central to plant-microbe interactions, as they enhance nutrient availability, stimulate root development and improve plant tolerance to environmental stresses [32]. Quantitative analysis revealed that *P. glycinae* (P2B) consistently produced higher levels of IAA than *P. aryabhattai* (P3A), suggesting a stronger potential to modulate root architecture. Elevated IAA production by rhizobacteria has been widely associated with increased root length, lateral root formation, and nutrient uptake efficiency, particularly under heavy metal stress where adaptive root growth is crucial [6, 33]. Phosphate solubilization assays indicated a time-dependent increase with P3A showing enhanced solubilization at later incubation stages. This suggests a dynamic phosphorus-mobilizing ability, likely mediated by organic acid production and pH reduction, which is essential for plant growth in phosphorus-deficient soils. Similar trends have been reported for *Priestia* and *Bacillus* related taxa, emphasizing their role in improving soil phosphorus bioavailability. Furthermore, higher ammonia production by P3A implies a greater contribution to nitrogen cycling in the rhizosphere, potentially supporting plant nitrogen nutrition. In contrast, siderophore production was more pronounced in P2A, reflecting its superior capacity to chelate iron and other micronutrients. Siderophores not only alleviate iron limitation but also reduce heavy metal toxicity by complexation, thereby indirectly protecting plants in contaminated soils [6, 33]. Both isolates demonstrated substantial tolerance to Ni,

Co, Cr and Cd, highlighting their adaptability to metal-stressed environments. Such tolerance is often attributed to mechanisms including metal sequestration, efflux pumps, enzymatic detoxification and extracellular binding, which collectively reduce metal bioavailability and toxicity [34]. The ability of these bacteria to persist under heavy metal stress is critical for maintaining effective plant-microbe associations in polluted soils and supports their role in phyto-stabilization and stress mitigation. In addition to PGP and metal tolerance traits, both isolates exhibited remarkable pyrene degradation efficiency, with P2B achieving 99% and P3A 98% degradation within 21 days. Pyrene, a high-molecular-weight PAH is known for its recalcitrant nature therefore, such high degradation rates indicate the metabolic versatility of the isolates. These findings are consistent with previous studies reporting PAH degradation by soil bacteria possessing aromatic ring-hydroxylating dioxygenases and related catabolic enzymes [35, 36]. The observed degradation efficiencies compare favorably with those reported for other environmental isolates highlighting the robustness of P2B and P3A under laboratory conditions.

5. Conclusion

The present study demonstrates that rhizobacterial isolates P2B and P3A possess distinct yet complementary plant growth-promoting traits coupled with pyrene degradation efficiency. A clear functional differentiation was observed with P2B strongly associated with IAA production and hydrocarbon degradation, while P3A exhibited superior nutrient solubilization and siderophore activity. These findings highlight the potential of these isolates, individually or as a consortium for enhancing plant growth and supporting sustainable bioremediation strategies in hydrocarbon-contaminated soils.

Declarations

Data Availability Statement

All data generated or analysed during this study are included in this published article and/or its supplementary information files.

Author Contributions

Meenakshi Shrivastav and Mahendra K Gupta contributed equally to the conception and design of the study. Meenakshi Shrivastav and Mir Sajad Rabani were responsible for writing the manuscript and performing data analysis. Mir Sajad Rabani and Mahendra K Gupta contributed to proofreading and editing. All authors reviewed and approved the final version of the manuscript.

Funding

The present research received no specific grant from any funding agency.

Competing Interests

The authors declare that there are no competing interests.

Ethical Approval and Consent to Participate

The plant sample collection was approved by the School of studies in Botany. The authors confirm that the collection of plant samples complies with the local and institutional guidelines of Jiwaji University with no further ethical approval required.

Consent to Publish

Consent to publish is not applicable

Clinical Trial

Clinic trial is not applicable

References

1. Fanai A, Bohia B, Lalremruati F, Lalhriatpuii N, Lalmuanpuii R, Singh PK. Plant growth promoting bacteria (PGPB)-induced plant adaptations to stresses: an updated review. Peer J. 2024;12:e17882.
2. Jmaili K, Bahlaouan B, Silkina A, Lahrairi M, Boutaleb N. Functional dynamics of Plant Growth-Promoting Bacteria (PGPB) in Adaptation to Abiotic Stress and Enhancement of Crop Productivity. Nat Built Social Environ Health. 2025;1(3):125–57.
3. Chaudhari D, Rangappa K, Das A, Layek J, Basavaraj S, Kandpal BK, Shouche Y, Rahi P. Pea (Pisum sativum L.) plant shapes its rhizosphere microbiome for nutrient uptake and stress amelioration in acidic soils of the North-East region of India. Front Microbiol. 2020;11:968.
4. Shrivastav M, Rabani MS, Pathak A, Sharma JK, Gupta C, Gupta MK. A Silent Threat: The Potential Consequences of Toxic Heavy Metals on Human Health. InGlobal Perspectives of Toxic Metals in Bio Environs: Volume 1: Environmental Impact, Ecotoxicology, Health Concerns, and Modelling 2025 Jul 12 (pp. 127–60). Cham: Springer Nature Switzerland.
5. Rabani MS, Habib A, Gupta MK. Polycyclic aromatic hydrocarbons: toxic effects and their bioremediation strategies. InBioremediation and Biotechnology, Vol 4: Techniques for Noxious Substances Remediation 2020 Oct 21 (pp. 65–105). Cham: Springer International Publishing.
6. Qin H, Wang Z, Sha W, Song S, Qin F, Zhang W. Role of plant-growth-promoting rhizobacteria in plant machinery for soil heavy metal detoxification. Microorganisms. 2024;12(4):700.
7. Sumathi K, Manian R. Degradation and inhibition kinetics of phenanthrene by Alcaligenes ammonioxydans,[VITRPS2] strain isolated from petroleum-contaminated soil. Discover Appl Sci. 2024;6(5):255.
8. Luo C, Guan G, Dai Y, Cai X, Huang Q, Li J, Zhang G. Determination of soil phenanthrene degradation through a fungal–bacterial consortium. Appl Environ Microbiol. 2024;90(6):e00662–24.
9. Zhou G, Qiao H, Liu Y, Yu X, Niu X. High phenanthrene degrading efficiency by different microbial compositions construction. Front Microbiol. 2024;15:1439216.

10. Rabani MS, Sharma R, Singh R, Gupta MK. Characterization and identification of naphthalene degrading bacteria isolated from petroleum contaminated sites and their possible use in bioremediation. Polycycl Aromat Compd. 2022;42(3):978–89.
11. Schoenborn L, Yates PS, Grinton BE, Hugenholtz P, Janssen PH. Liquid serial dilution is inferior to solid media for isolation of cultures representative of the phylum-level diversity of soil bacteria. Appl Environ Microbiol. 2004;70(7):4363–6.
12. Gordon SA, Weber RP. Colorimetric estimation of indoleacetic acid. Plant Physiol. 1951;26(1):192.
13. Patten CL, Glick BR. Role of Pseudomonas putida indoleacetic acid in development of the host plant root system. Appl Environ Microbiol. 2002;68(8):3795–801.
14. Pikovskaya R, Pikovskaya RI, Pikovskaya RI. In. Mobilization of phosphorus in soil in connection with the vital activity of some microbial species. 1948.
15. Fankem H, Nwaga D, Deubel A, Dieng L, Merbach W, Etoa FX. Occurrence and functioning of phosphate solubilizing microorganisms from oil palm tree (Elaeis guineensis) rhizosphere in Cameroon. Afr J Biotechnol. 2006;5(24).
16. Nautiyal CS. An efficient microbiological growth medium for screening phosphate solubilizing microorganisms. FEMS Microbiol Lett. 1999;170(1):265–70.
17. Schwyn B, Neilands J. Universal chemical assay for the detection and determination of siderophores. Anal Biochem. 1987;160(1):47–56.
18. Payne SM. Detection, isolation, and characterization of siderophores. Methods Enzymol. 1994;235:329–44.
19. Lorck H. Production of hydrocyanic acid by bacteria. Physiol Plant. 1948;1(2).
20. Cappuccino JG, Sherman N. Microbiology: a laboratory manual. San Francisco: Pearson/Benjamin Cummings; 2005.
21. Saravanan VS, Madhaiyan M, Thangaraju M. Solubilization of zinc compounds by the diazotrophic, plant growth promoting bacterium Gluconacetobacter diazotrophicus. Chemosphere. 2007;66(9):1794–8.
22. Baskar B, Prabakaran P. Assessment of nitrogen fixing bacterial community present in the rhizosphere of Avicennia marina. Indian J Geo-Mar Sci. 2015;44(3):318–22.
23. Kumar A, Kumar A, Devi S, Patil S, Payal C, Negi S. Isolation, screening and characterization of bacteria from Rhizospheric soils for different plant growth promotion (PGP) activities: an in vitro study. Recent Res Sci Technol. 2012;4(1):1–5.
24. Singh A, Kumar A, Yadav S, Singh IK. Reactive oxygen species-mediated signaling during abiotic stress. Plant gene. 2019;18:100173.
25. Gupta S, Kaushal R, Spehia RS, Pathania SS, Sharma V. Productivity of capsicum influenced by conjoint application of isolated indigenous PGPR and chemical fertilizers. J Plant Nutr. 2017;40(7):921–7.

26. Hassan TU, Bano A, Naz I. Alleviation of heavy metals toxicity by the application of plant growth promoting rhizobacteria and effects on wheat grown in saline sodic field. Int J Phytoremediation. 2017;19(6):522–9.
27. Dhar K, Panneerselvan L, Venkateswarlu K, Megharaj M. Efficient bioremediation of PAHs-contaminated soils by a methylotrophic enrichment culture. Biodegradation. 2022;33(6):575–91.
28. Ghosh P, Thakur IS. Biodegradation of pyrene by Pseudomonas sp. ISTPY2 isolated from landfill soil: Process optimisation using Box-Behnken design model. Bioresource Technol Rep. 2019;8:100329.
29. Ma J, Xu L, Jia L. Characterization of pyrene degradation by Pseudomonas sp. strain Jpyr-1 isolated from active sewage sludge. Bioresour Technol. 2013;140:15–21.
30. Holt JG, Krieg NR, Sneath PHA, Staley JT, Williams ST. Bergey's Manual of Determinative Bacteriology. 9th ed. Baltimore: Williams & Wilkins; 1994.
31. Muratova A, Golubev S, Romanova V, Sungurtseva I, Nurzhanova A. Effect of heavy-metal-resistant PGPR inoculants on growth, rhizosphere microbiome and remediation potential of miscanthus× giganteus in Zinc-contaminated Soil. Microorganisms. 2023;11(6):1516.
32. Sun Y, Yang Z, Zhang C, Xia J, Li Y, Liu X, Sun L, Tan S. Indole-3-propionic acid regulates lateral root development by targeting auxin signaling in Arabidopsis. Iscience. 2024;27(7).
33. Sharma N, Sharma G, Kour S, Chadha BS, Ohri P. Unravelling the role of plant growth promoting rhizobacteria in boosting plant growth and phytoremediation of heavy metals. Appl Soil Ecol. 2024;199:105416.
34. Riseh RS, Vazvani MG, Hajabdollahi N, Thakur VK. Bioremediation of heavy metals by rhizobacteria. Appl Biochem Biotechnol. 2023;195(8):4689–711.
35. Song Q, Song X, Deng X, Luo J, Wang J, Min K, Song R. Effects of plant growth promoting Rhizobacteria microbial on the growth, rhizosphere soil properties, and bacterial community of Pinus sylvestris var. mongolica seedlings. Scand J For Res. 2021;36(4):249–62.
36. Umar ZD, Abd NA, Zulkifli SZ, Mustafa M. Efficiency of polycyclic aromatic hydrocarbons (PAHs) degrading consortium in resisting heavy metals during PAHs degradation. Int J Environ. 2018;7(1):14–27.

Figures

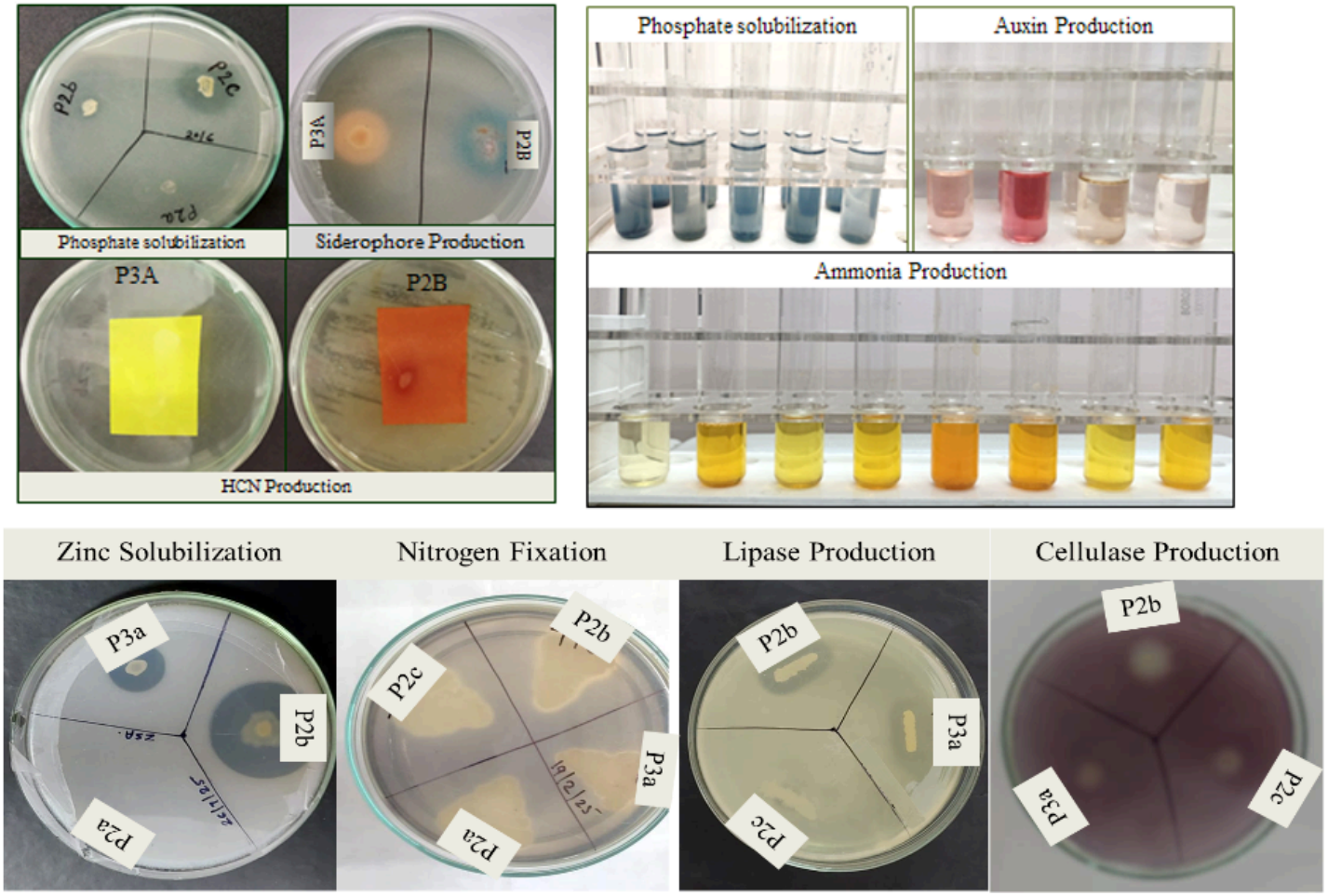


Figure 1

Qualitative plant growth promoting traits assay

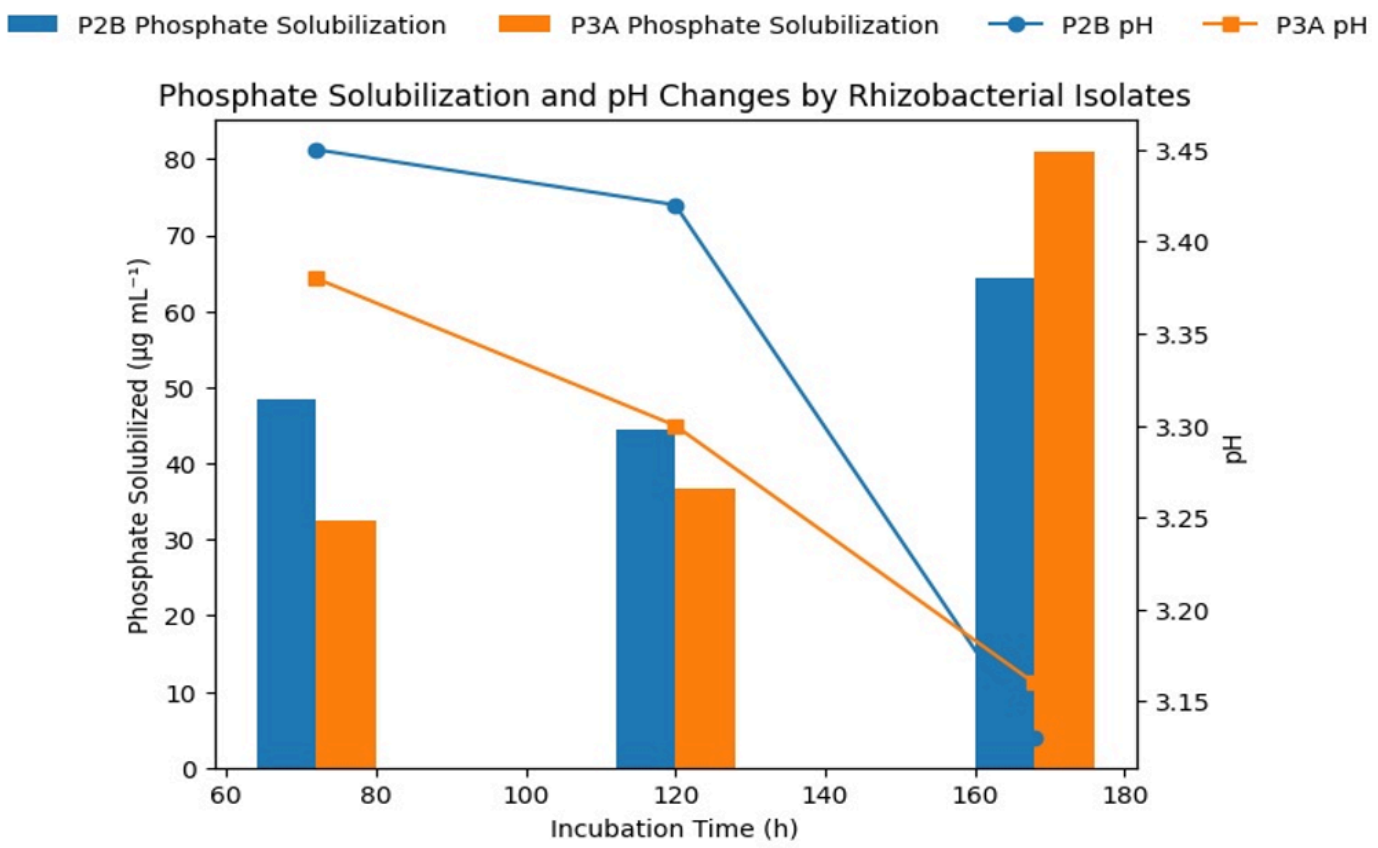


Figure 2

Phosphate solubilization and associated pH changes by rhizobacterial isolates P2B and P3A during incubation at 72, 120 and 168 h. Bars represent phosphate solubilization (µg mL^{-1}), while lines indicate corresponding pH variation.

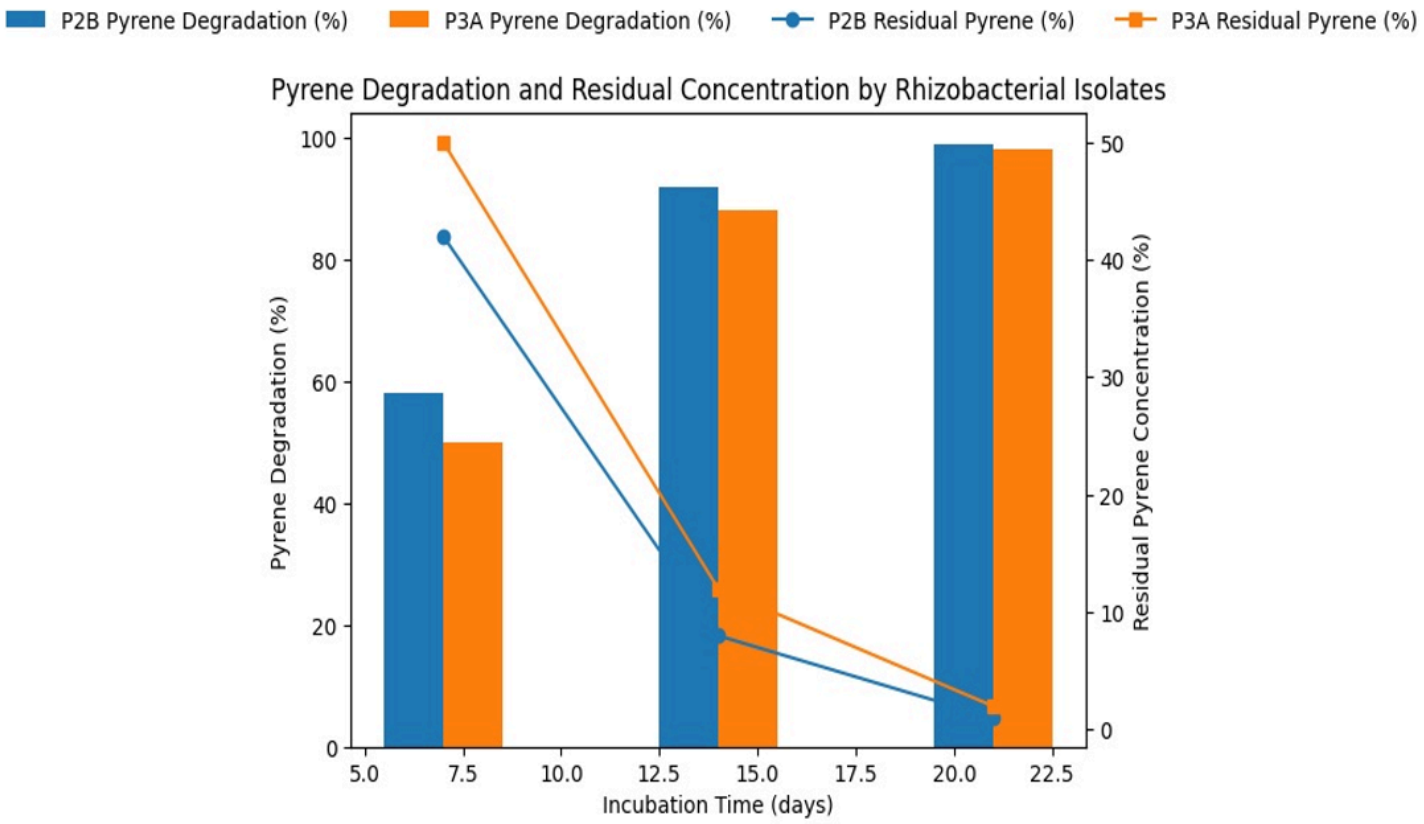


Figure 3

Pyrene degradation efficiency and corresponding residual pyrene concentration by rhizobacterial isolates P2B and P3A during incubation (at 50 mg L^{-1}). Bars represent percentage degradation of pyrene, while lines indicate residual pyrene concentration over 7, 14 and 21 days of incubation.

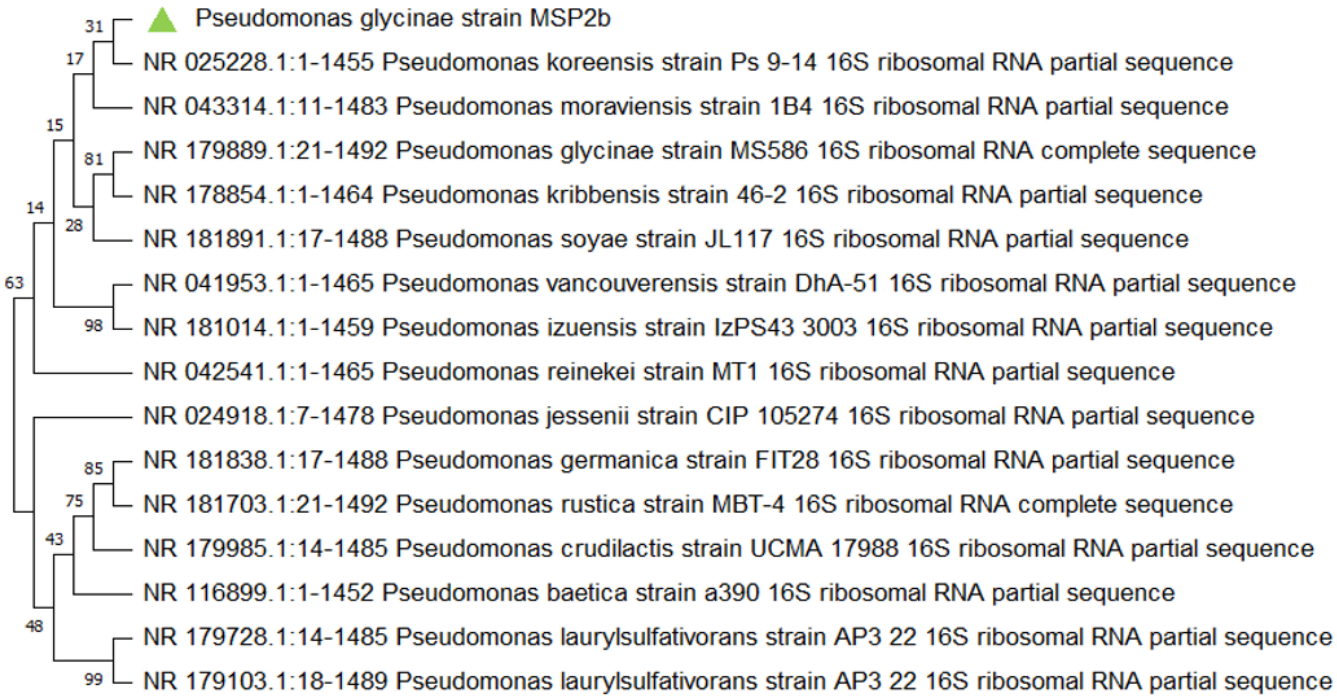


Figure 4

Phylogenetic tree of *Pseudomonas glycinae* strain MSP2B constructed by neighbor joining method

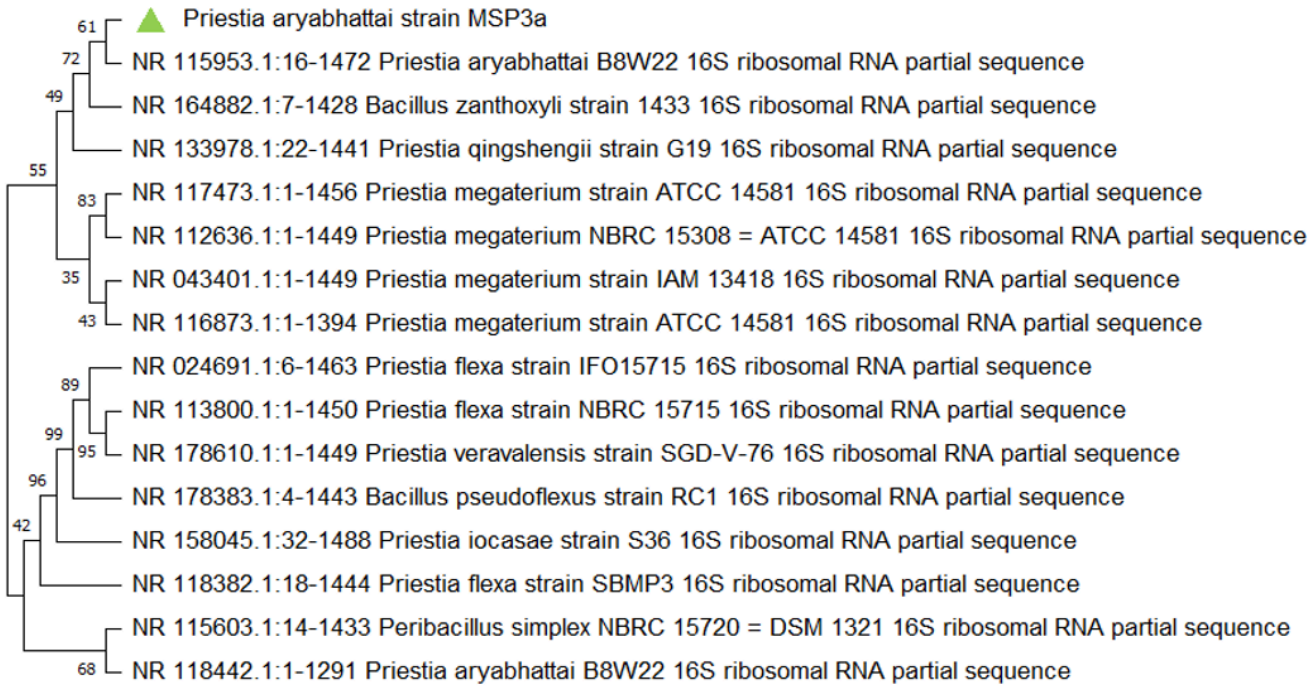


Figure 5

Phylogenetic tree of *Priestiaary abhattai* strain MSP3A constructed by neighbor joining method

Supplementary Files

This is a list of supplementary files associated with this preprint. Click to download.

- flatfileP2B.txt
- flatfileP3A.txt